Materials Transactions, Vol. 51, No. 12 (2010) pp. 2236 to 2242

Effects of Steel Coatings on Electrode Life in Resistance Spot Welding of Galvannealed Steel Sheets

X. Hu[1,2], G. Zou[2,3], S. J. Dong[1], M. Y. Lee[4], J. P. Jung[5,*] and Y. Zhou[2]

[1]*School of Mechanical Engineering, Hubei University of Technology, Wuhan 430068, P. R. China*
[2]*Center for Advanced Materials Joining, University of Waterloo, Waterloo, ON N2L 3G1, Canada*
[3]*Department of Mechanical Engineering, Tsinghua University, Beijing 100084, P. R. China*
[4]*Research Institute of Industrial Science & Technology, Pohang 790-330, Korea*
[5]*Department of Materials Science and Engineering, University of Seoul, Seoul 130-743, Korea*

The effects of different galvannealed (GA) coatings, containing Fe varying from 7.0 to 11.4 mass%, on steel sheets on the electrode life in resistance spot welding (RSW) have been investigated with metallurgical analysis of the coating microstructures and properties, and the surfaces and cross-sections of failed electrodes. The results showed that the electrode life in RSW of GA steel with 11.4 mass% Fe in coating was 110% higher than that with coatings containing 7.0 or 9.6 mass% Fe. The improvement was believed to be caused by the build-up of a Fe-rich alloy layer on the electrode surface, which could serve as a barrier to prevent copper loss from the electrode surfaces to the steel sheets, thus reducing the growth rate of the electrode tip face diameters. In addition, higher Fe content in the coating resulted in increased contact resistance and hence a lower welding current needed in RSW. [doi:10.2320/matertrans.M2010239]

(Received July 21, 2010; Accepted August 26, 2010; Published October 27, 2010)

Keywords: *resistance spot welding, galvannealed steel, electrode life, coating composition and microstructures*

1. Introduction

Resistance spot welding has been used for various fields from an auto industry[1)] to a medical area.[2)] In the automotive industry, galvannealed (GA) steel sheet is used for both exposed and internal body parts because of its superior corrosion resistance and its good weldability and paintability.[3,4)] Galvannealed coatings are essentially diffusion layers containing Fe-Zn intermetallic phases formed between molten Zn and steel substrates at annealing temperatures around 500°C. Depending on the heat treatment conditions, there are four intermetallic Fe-Zn compounds, i.e., zeta (ξ), delta (δ) and two gamma (Γ, Γ_1) phases that may be observed,[5)] as can also be inferred from the phase diagram (Fig. 1). For example, Long[6)] indicated that a low-iron coating (about 10.4 mass% Fe) had a 2–3 µm of ξ phase, 3–4 µm of δ phase and 1 µm of Γ phase, while a coating of higher iron content (13.3 mass% Fe) had a Γ-layer 1–2 µm thick, a δ-layer 4~5 µm thick, and a very thin ξ-layer on the galvannealed coating surface, based only on scanning electron microscopy (SEM) and energy dispersive spectrometry (EDS) analysis. But the exact microstructure of the coatings (type and thickness of the intermetallic layers, etc.) was very sensitive to the heat treating conditions, such as heating rate, hold temperature and time, and cooling rate of the galvannealing treatment.[3,5)] Although not represented in Fig. 1, η phase is a solid solution of Fe in Zn with solubility limit of 0.03 mass%. The detailed characteristics and microhardness of these intermetallic compounds and pure phase are summarized in Table 1.[4–8)]

Resistance spot welding (RSW) has been the primary joining technique for automotive body-in-white assembly since the 1930s.[9)] An important factor in RSW of Zn-coated steel is electrode life, that is, a limit to the number of spot welds that can be made before corrective action is required.[10)] Electrode life is generally defined as the number of welds that can be made, without dressing the electrode tips, before the weld size falls below an acceptable level. Electrode tip wear, resulting in electrode tip face growth, has been suggested as the dominant process that limits electrode life in RSW of Zn-coated steel.[11,12)] When welding zinc-coated steel and other alloys, the alloying and local bonding between electrodes and sheets often results in the removal of Cu from the electrode tip surface (and hence electrode wear) as evidenced by Cu being found on the surface of the welds.[13–16)] Obviously, it is helpful to increase electrode life by preventing alloying between electrodes and sheets. For example, Dong and Zhou[17,18)] investigated the effects of a TiC composite coating on the electrode surfaces on electrode tip degradation in

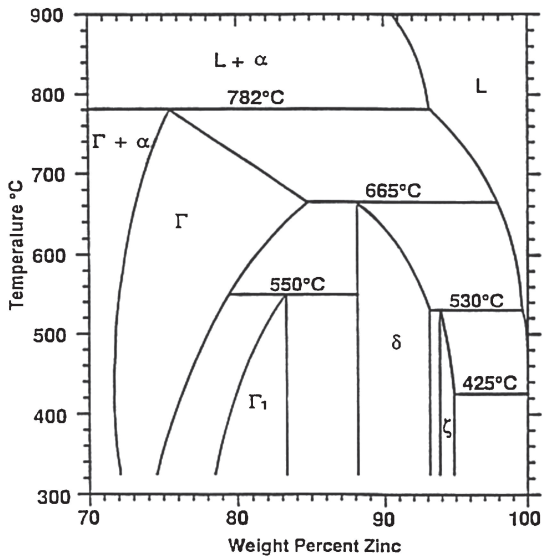

Fig. 1 Zinc rich corner of the Fe-Zn binary phase diagram.[7)]

*Corresponding author, E-mail: jpjung@uos.ac.kr

Table 1 Fe-Zn phase characteristics.[4–9)]

Phase	Formula	Crystal structure	Fe content (mass%)	Melting points (T/°C)	VHN (25 mg)
η	Zn	Hexagonal	~100	419.4	52
ξ	$FeZn_{13}$	Monoclinic	5.2~6.1	530	208
δ	$FeZn_{10}$~$FeZn_7$	Hexagonal	7.0~11.5	672	358
Γ_1	Fe_5Zn_{21}~$Fe_{11}Zn_{40}$	FCC	17.0~22.0	NA*	505
Γ	Fe_3Zn_{10}~$FeZn_3$	BCC	24.0~31.0	782	326
α-Fe	Fe	BCC	~100	1538	104

*Note: Γ_1 phase transforms to the $\Gamma + \delta$ mixed phases at 550°C.

resistance welding of nickel-plated steel, and indicated that the electrode coating could serve as a barrier layer to reduce the Cu loss from the electrode, increasing electrode life.

Pickett *et al.*,[19)] in an investigation of electrode life in RSW of GA steels with coatings containing different Fe contents, have shown that the electrode life was increased by two-fold when Fe content increased from 8 to 10 mass% and further increased when Fe increased to 13 mass%. But, unfortunately, the electrode life tests were arbitrarily stopped at 10,000 welds for 13 mass% Fe so that the exact improvement was not quantified. Also the reason for the increase in electrode life was not discussed. The present work has aimed at clarifying the effects of steel coatings on electrode life in RSW of GA steels and the mechanism of improving electrode life by increasing Fe content in the coating.

2. Experimental

The steel substrate used in this work was 0.7 mm in thickness with chemical composition, in mass%, as C = 0.003, Si = 0.01, Mn = 0.09, P = 0.009, S = 0.005, Al = 0.051, Cr = 0.012, Mo = 0.003, Cu = 0.018, Ni = 0.008, Sn = 0.003, V = 0.002, Nb = 0.014, Ti = 0.026. The coating thickness on both steel sides and the nominal Fe content in the coatings are 9.2, 8.9 and 8.5 µm, 7.0, 9.6 and 11.4 mass%, respectively for steels #1, #2 and #3, which were the averages of 10 measurements each by a JEOL JSM-6460 scanning electron microscope (SEM) equipped with energy-dispersive spectrometer (EDS) on the cross-sections of steel sheets. X-ray diffraction (XRD) analysis was conducted using a Rigaku AFC8 power X-ray diffractometer using Cu K_α radiation. Micro-hardness of steel coatings was measured using a HMV 2000 Vickers hardness tester at 5 g load on prepared metallographic cross-section samples.

All spot welds were produced by an air operated stationary single phase alternating current (AC) RSW machine of 250 kVA rating at 60 Hz. The electrodes used in this work were RWMA Group A, Class II, Cu-Cr-Zr domed-flat nose, female caps with nominal tip face diameter of 4.8 mm ± 0.5 mm. Electrode force (2000 N), weld time (11 cycles), cooling water flow (4 L/min), welding rate (25 welds/min), and short (5 cycles) and long hold time (90 cycles), specified by recommended practices of the AWS standard, AWS/ANSI/SAE D8.9-97,[20)] were used in this work. Based on the standard, electrode life can be determined in an endurance test following a weld size stabilization test (to compensate for the dynamic behavior of welding current versus weld size that occurs when making welds with new electrodes) and a current test (to determine the welding current that will be used in the endurance test), all on the same set of two electrodes.[20)]

In the stabilization tests, the initial current was selected to be 7000 A, based on the AWS standard on 0.7-mm-thick zinc-alloy coated steel sheets. Stabilization weld-button size (SWS) is defined as 90 percent of the dressed tip face diameter without expulsion or severe sticking,[20)] which was 4.4 mm in this work based on 0.9 × 4.9 mm rounded to the closest 0.1 mm (4.9 mm is the average of measured initial tip face sizes Using the carbon imprint technique,[21)] which were 4.90, 4.91 and 4.88 mm for the electrodes for steels #1, #2 and #3 respectively). Weld (button) size was determined by the button left on one steel sheet after peel testing.[20)] Once the total welds reached 250, the stabilization test ended and the same set of electrodes moved on to the current test.[20)]

At the start of the current test, the initial current I_0 should be sufficiently low to produce a weld that is at least 0.5 mm smaller than the minimum weld size (MWS), defined as $4\sqrt{t}$ (t is the thickness of the coated steel sheet), i.e., MWS = $4\sqrt{0.7} = 3.35$ mm in this work. This initial current was selected to be 8300 A, 7300 A and 7200 A for steels #1, #2 and #3, respectively, based on the weld size and welding current data from the stabilization test. The final currents, based on when expulsion or severe electrode sticking occurs,[20)] was determined to be 9200, 8700, 8500 A for steels #1, #2 and #3, respectively. The total welds made in the stabilization and current tests were 274, 288 and 288, respectively for steels #1, #2 and #3.

The welding current for the endurance test is set as the final current less 200 A, i.e., 9000 A, 8500 A and 8300 A for steels #1, #2 and #3, respectively. According to the AWS standard,[20)] when the weld button size drops to a value lower than MWS, i.e., 3.35 mm, the number of welds made is deemed endurance life. In this work, electrode life is taken as the sum of total welds made in the stabilization, current and endurance tests.

Figure 2 shows the carbon imprints of electrode tip faces at the start of the stabilization test, and the start and end of the endurance test with electrode tip face diameter as 4.91, 4.88 and 4.90 mm respectively for steels #1, #2, and #3 after the stabilization and current tests. This indicates that no significant change took place in the electrode tip morphology and size before and after the stabilization and current tests. Only one pair of electrodes for each type of steel coating was tested because of the limited supply of steel sheets. But fortunately the electrode life tests using the AWS standard showed very good consistency in RSW of these GA steels.[19)]

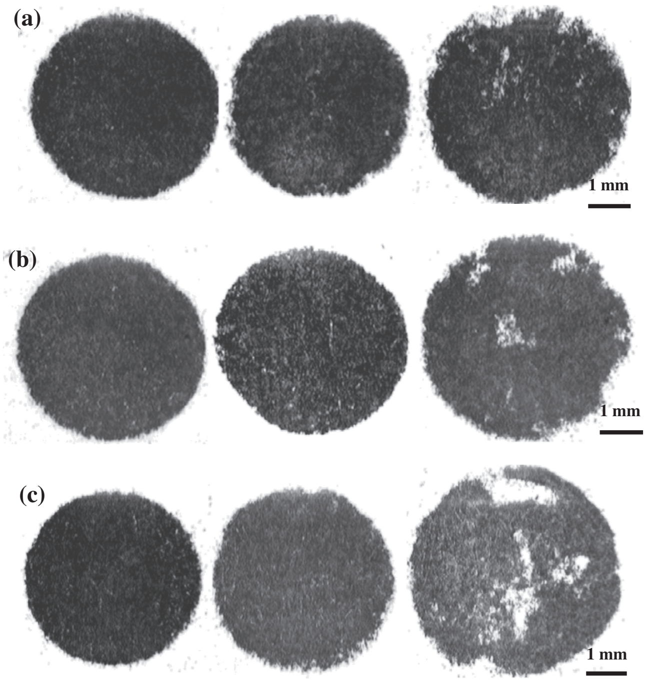

Fig. 2 Carbon imprints of electrode tip faces for steels (a) #1, (b) #2 and (c) #3 at the start (left) the end (centre) of stabilization tests and at the end of endurance test (right).

The contact resistances between electrode and steel sheet, and between steel sheets, were measured under weld force (2000 N) without welding current. Data reported are averages of fifteen replicate measurements using a digital four-point low-resistance ohmmeter.

3. Results

3.1 Steel coating microstructure and hardness

In Fig. 3, the SEM cross-sections of the Zn-Fe coatings on the steel sheets are shown, in which the compositions of the labeled regions were determined by EDS as reported in Table 2. Steel #1 was found to have a three-layer structure marked as layers A, B and C, with thicknesses around 1∼2, 4∼5 and 2∼3 µm respectively, and compositions of Zn-1.2 mass%Fe, Zn-5.5 mass%Fe and Zn-10.1 mass%Fe

Table 2 EDS results of labeled areas in Fig. 3 (mass%).

	Steel #1			*Steel #2*		*Steel #3*		
	A	B	C	B	C	C	D	E
Fe	1.2	5.5	10.1	6.7	10.5	10.4	14.5	27.7
Zn	98.8	94.5	89.9	93.3	89.5	89.6	85.5	72.3
Possible phases	η	ξ	δ	ξ	δ	δ	Γ_1	Γ

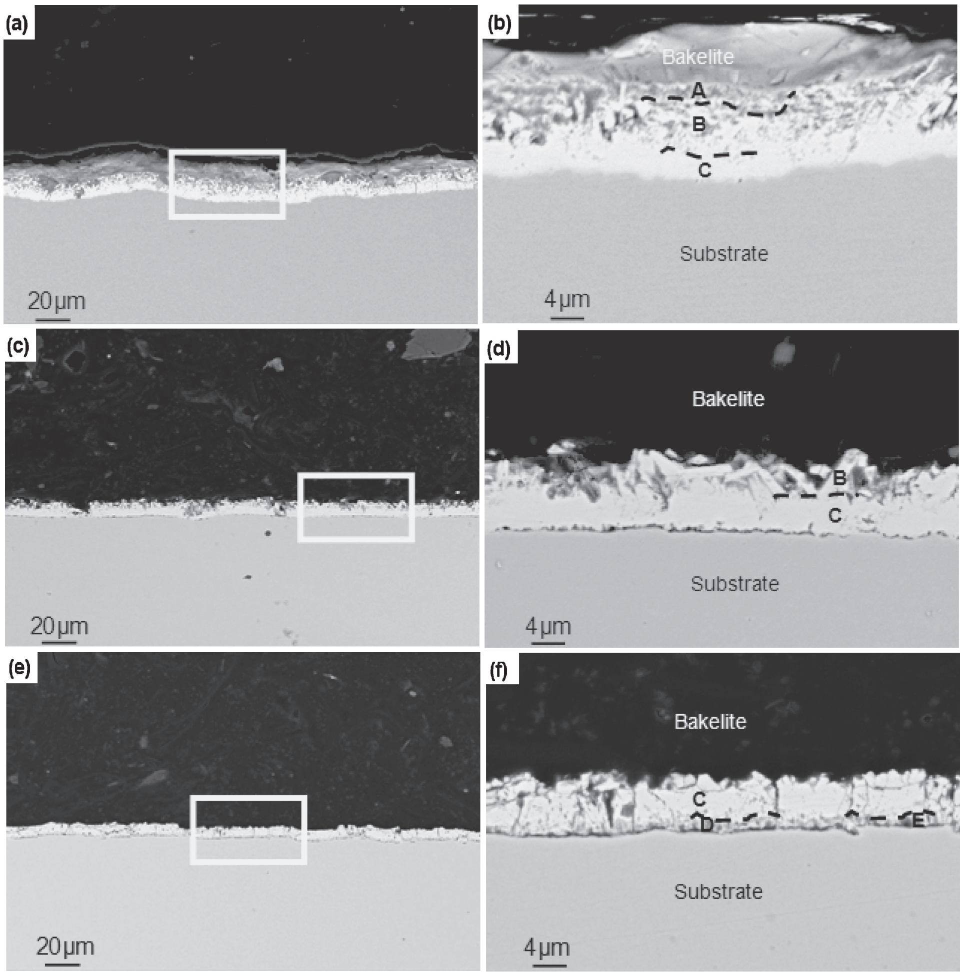

Fig. 3 SEM backscatter images at lower and higher magnification of highlighted areas for steels #1 (a) and (b), #2 (c) and (d), and #3 (e) and (f), respectively.

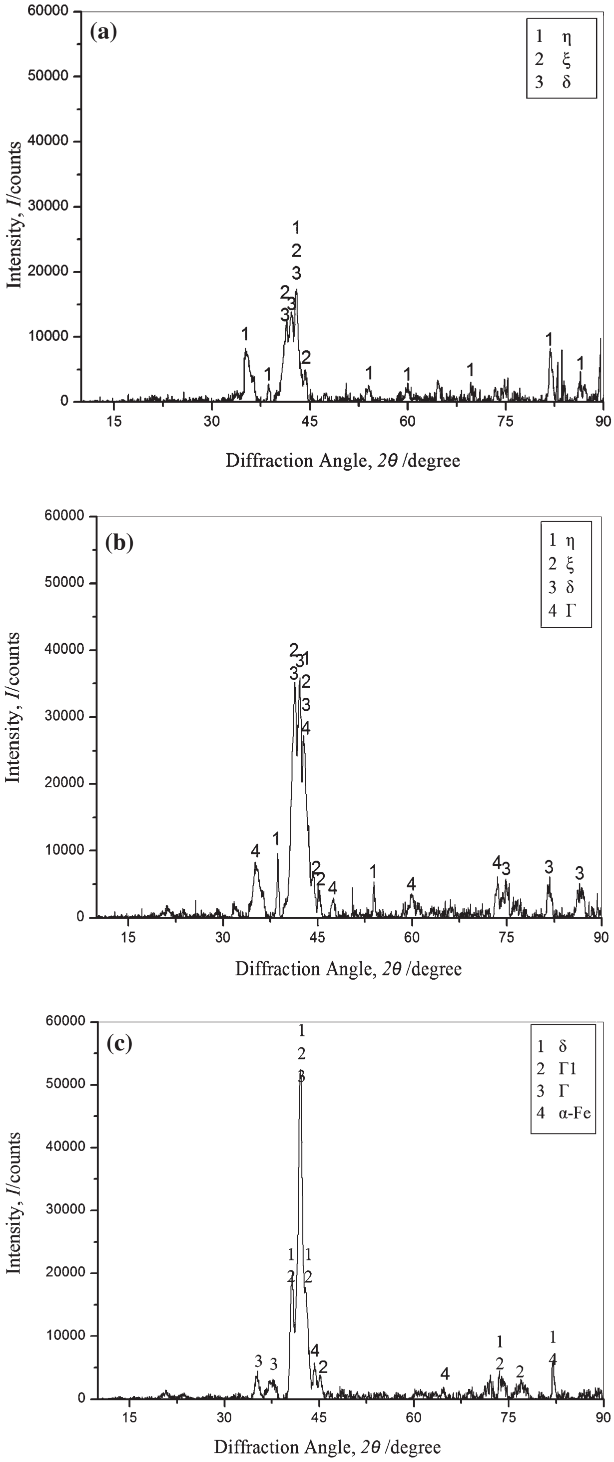

Fig. 4 XRD spectra of the coating surfaces of steels #1 (a), #2 (b) and #3 (c).

(Table 2). Although the inherent accuracy of EDS analysis for these very thin layers is not high, a comparison of Table 2 with the phase diagram (Fig. 1 and Table 1) indicates that possible phases of the A, B and C layers were η, ξ and δ, respectively. These were confirmed by the XRD analysis (Fig. 4(a)).

The coating on steel #2 displayed a two-layer structure as shown in Fig. 3(c) and (d). The outer layer (B) had a saw-toothed shape with around 3~4 µm thickness, and the inner layer (C) was around 4~5 µm in thickness. The EDS analysis

Table 3 Coating microhardness and contact resistance.

Steel sheets	Hardness (H/H_V 5 g)	Contact resistance between electrode and sheet ($\rho/\mu\Omega$)	Contact resistance between sheets ($\rho/\mu\Omega$)
#1	159.1 ± 4.5	9.5 ± 2.3	20.8 ± 3.5
#2	253.3 ± 6.4	10.1 ± 2.5	26.8 ± 3.7
#3	373.5 ± 10.6	34.3 ± 3.6	50.7 ± 4.5

indicated that the compositions of B and C layers were Zn-6.7 mass%Fe and Zn-10.5 mass%Fe, respectively, which were confirmed by the XRD analysis (Fig. 4(b)) to be ξ and δ phases. Although the η and Γ phases were detected from the XRD spectra in Fig. 4(b), these were not found in the EDS results. A possible reason could be that these layers might be very thin and/or discontinuous, especially for the Γ phases between the steel substrate and δ phase layer.[7)]

From the SEM/EDS and XRD results, as shown in Figs. 3 and 4, it was noted that the coating of steel #3 consisted mainly of δ layer with a thickness of 6~7 µm, marked by letter "C" in Fig. 3(f). Between the δ layer and substrate, a thinner layer about 1~2 µm thick was seen. From Table 2 and XRD results in Fig. 4(c), the marks of "D" and "E" in Fig. 3(f) corresponded to compositions of Zn-14.5 mass%Fe and Zn-27.7 mass%Fe in the thinner layer, respectively, thus it was indicated that the microstructure in the thinner layer was a Γ_1 and Γ mixture.

Considering that steel coating microstructure can be greatly influenced by the heat treatment conditions,[3,5)] the observations in this work are in general agreement with the literature. For example, Pickett *et al.*[19)] indicated in a study of RSW of GA steels that ξ plus a thin discontinuous layer of Γ phase existed at 8 mass% Fe, δ and ξ plus a thin discontinuous layer of Γ phases at 10 mass% Fe, and δ phase plus a relatively thick continuous layer of Γ phase was present at 13 mass% Fe, although only SEM/EDS analysis was conducted. As the Fe content in GA steel coatings increase, the thickness of the δ layer increases, Γ and Γ_1 phases start to form and grow, and the η layer reduces or even disappears.[5)]

Table 3 shows the microhardness of these steel coatings and the contact resistance of electrode/sheet and sheet/sheet interfaces. It is clear that higher Fe content increased the hardness of the coating on the steel surface because of the thicker and harder surface layers containing δ, Γ_1 and Γ phases (Table 1), which resulted in the highest hardness in the coating on steel #3. Harder coating hardness resulted in higher contact resistance, especially for steel #3, as shown in Table 3. Friedman *et al.*[22)] indicated that when welding galvannealed steel, high coating hardness would result in decreased interface contact area under the identical electrode force. Both smaller contact area and higher surface hardness increases contact resistance.[15,23)] On the contrary, the lower hardness η phase (about 50 H_V, Table 1) in the coating reduced coating hardness and hence contact resistance for steel #1. Higher contact resistance also resulted in lower welding current required to obtain the same button size for steel #3, which is consistent with the literature.[15,22,24)] The static contact resistance in the Table 3 is the starting point of the dynamic resistance in actual welding. Although it

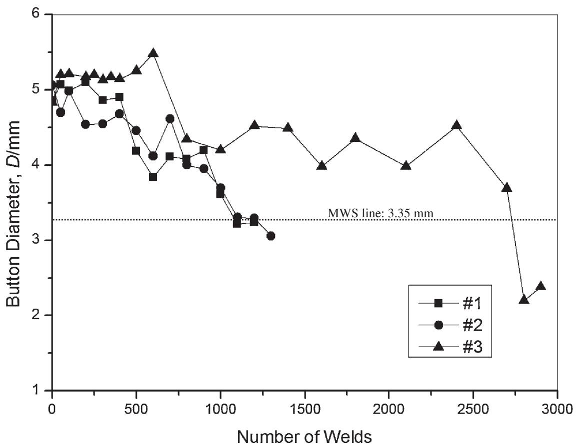

Fig. 5 Button diameter versus the number of welds during endurance test.

cannot be used to replace dynamic resistance, but can give a rough indication of the relative values of the dynamic resistance.[25)]

3.2 Electrode life

The relations between button size and number of welds during the endurance tests are shown in Fig. 5. According to the AWS standard,[20)] when the weld button size becomes smaller than MWS, 3.35 mm, as illustrated by a dashed line in Fig. 5, the number of welds is deemed endurance life. Electrode life is taken as the sum of welds made in the stabilization and current tests, and the endurance tests. Therefore, the electrode lives of steels #1, #2 and #3 are 1349, 1388 and 2988 welds, respectively. This indicates that the electrode life of the GA steel with a coating containing 11.4 mass% Fe increased by 110% compared to that of the steel with 9.6 mass% Fe at the coating, while the electrode life was similar when the Fe content increased from 7.0 mass% to 9.6 mass%. The three dimensional changes of the electrode tip shape during the endurance tests were not significant in this study.

4. Discussion

The backscattered SEM images of the cross-sections of failed electrodes in RSW of steels #1, #2 and #3 are shown in Fig. 6. The EDS results of labeled areas, i.e., A in steel #1, A+B in steel #2, A+B+C+D+E in steel #3, are shown in Table 4. It was observed that the A zone contained mainly Cu and Zn; B and C zones contained Fe, Zn and Cu; D and E zones contained Fe and Zn. On the other hand, XRD analysis (Fig. 7) indicated Cu-Zn and Fe-Cu phases; Cu, Zn, Cu-Zn, Cu-Fe, and Fe-Zn phases; and Cu-Zn and Fe-Zn phases on the surface of failed electrodes in steel #1, #2, and #3, respectively. Comparing Figs. 6, 7 and Table 4, it was noted that the main difference between the electrodes in steels #1, #2 and #3 was the outermost, continuous layers of Fe rich phases on the steel #3 electrodes. The Fe on the electrode surface must come from the steel substrates because of very negligible Fe content in the Cu electrode.

It has been proposed by Dilthey *et al.*[26)] that the material transfer mechanism follows one of three possible scenarios in RSW of Al sheets, i.e.: (1) the resultant local bond, mainly

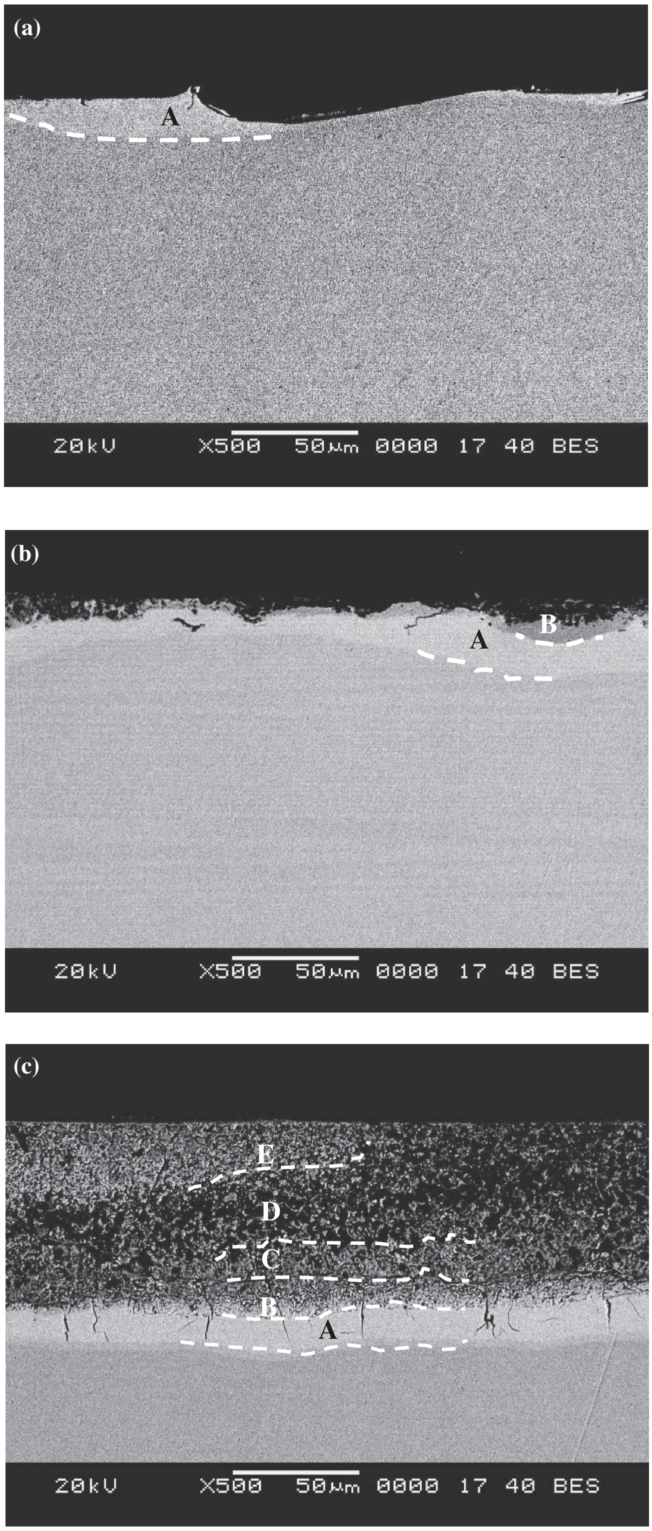

Fig. 6 SEM backscatter image of electrode cross-sections at the end of life for steels #1 (a), #2 (b) and #3 (c) #3.

Table 4 Chemical elements in labeled areas in Fig. 6 (mass%).

	#1	#2		#3				
	A	A	B	A	B	C	D	E
Fe	0.3	0.5	71.3	0.6	5.4	23.0	34.6	55.1
Cu	81.3	51.1	5.9	31.3	22.6	5.9	0	0
Zn	18.4	48.4	39.0	68.1	72.0	71.1	65.4	44.9

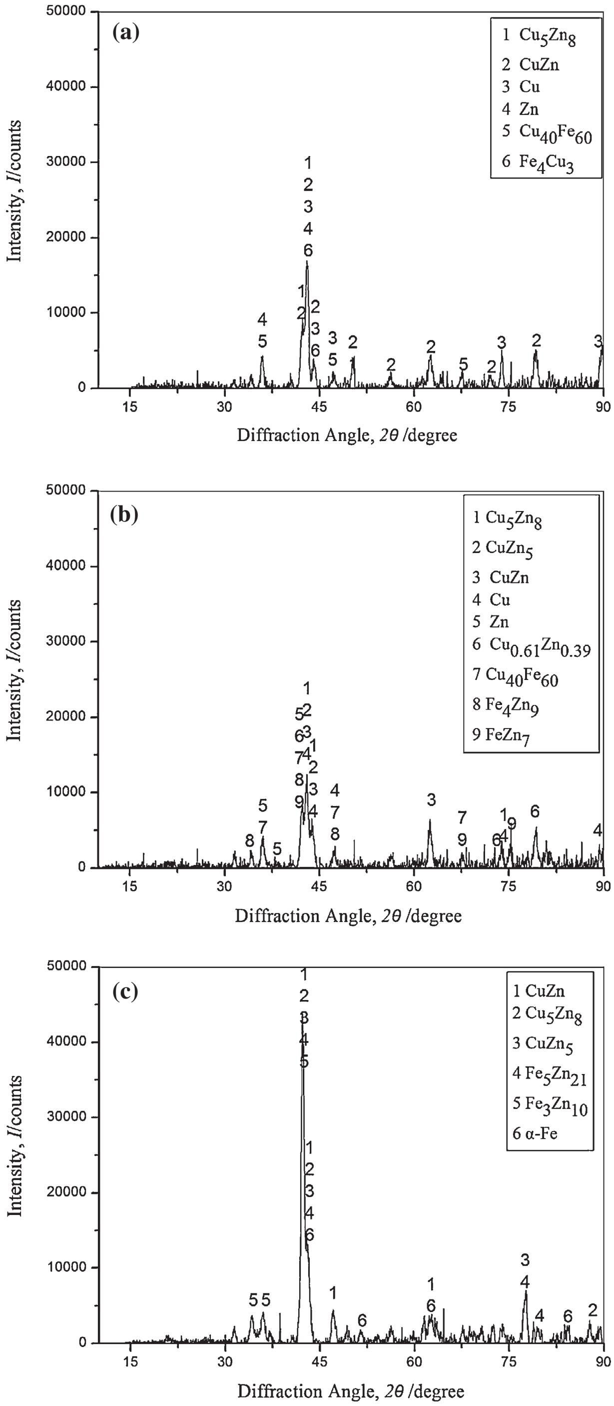

Fig. 7 XRD spectra of electrode surfaces at the end of life for steels #1 (a), #2 (b) and #3 (c).

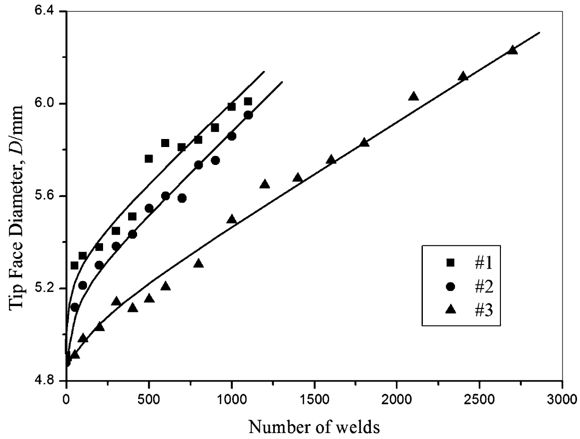

Fig. 8 Electrode tip face diameter versus the number of welds during endurance test.

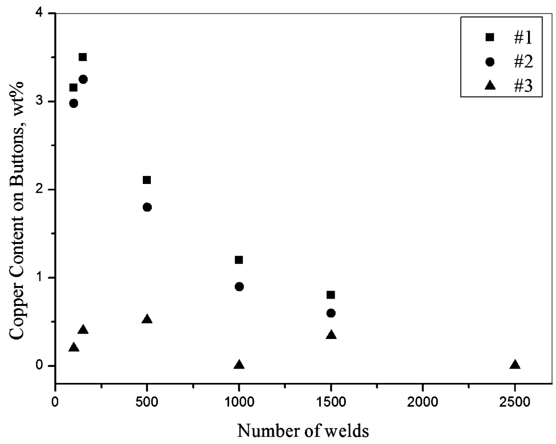

Fig. 9 Copper content on the button (weld) surfaces.

formed of Al-Cu alloy, between the Cu electrode and Al substrate during welding is entirely pulled from the electrode surface and accumulates on the Al sheet, (2) the entire Al-Cu alloy breaks away from the substrate and transfers onto the electrode surface, and (3) the Al-Cu alloy breaks internally, with part of the alloy sticking on the substrate and the rest on the electrode surface. While first and third scenarios have been confirmed in RSW of Al-alloy 5182,[19] the first appears to be the main material transfer mechanism in RSW of Zn-coated and other alloys, and removal of Cu from the electrode tip surfaces is therefore the reason of increased electrode wear.[13–16]

However, in the present study, it appears that the material transfer in RSW of steel #3 follows mainly the second scenario, i.e., the alloying between the steel coating and electrode breaks from the steel sheet and accumulates on the electrodes, as evidenced by Fe pick up on the electrode surfaces (Table 4, and Fig. 6 and 7). This results in formation of Fe rich layers on the electrode surface, which in turn can serve as a barrier to prevent further interaction between the Cu electrode and steel coating, hence eliminating the removal of Cu from the electrodes. This can also be seen from the preservation of Cu-Zn alloy layers between the Fe rich layers and copper alloy substrate (Fig. 6(c)) as comparing to steels #1 and #2 (Fig. 6(a) and (b)). This Fe-rich barrier is similar to the TiC composite coating applied on electrode tip surfaces to improve electrode life.[17,18] But the accumulation of the Fe-rich layer will also contribute to the growth of the tip face diameter, and eventually reduce the current density and fail the electrode.

On the other hand, electrode degradation in RSW of steels #1 and #2 follows mainly the first material transfer scenario proposed by Dilthey *et al.*[26] The continuous breaking off of Cu-Zn alloy from the electrodes results in fast removal of Cu and hence growth in electrode tip face diameter and reduced electrode life (Fig. 8). This is can be seen from Fig. 9 in which the mean copper contents on the steel surfaces of welds are much higher in steels #1 and #2 than in steel #3.

5. Conclusions

An experimental study was carried out to detail the effects of coating composition and microstructure on electrode life in resistance spot welding (RSW) of galvannealed steel sheets. The analysis of the results has led to the following conclusions:

(1) In GA steels, the coating containing 11.4% Fe included layers of mixed Γ and Γ_1 phases, and δ phase, while the coating containing 9.6% Fe included δ and ξ phases and the coating containing 7.0% Fe included δ, ξ and η phases. Higher Fe content in the coating resulted in higher coating hardness and hence higher contact resistance between steel sheets and also reduced welding current required to obtain the same weld size in RSW.

(2) The electrode life when welding GA steel with coating containing 11.4 mass% Fe was increased by 110% compared to that with coating containing 9.6 mass% Fe while electrode life was similar when the Fe content in coating increased from 7.0 mass% to 9.6 mass%.

(3) The improvement in electrode life was believed to be caused by the build-up of Fe-rich alloy layers on the electrode surface, which could serve as a barrier to prevent copper loss from the electrode surfaces to the steel sheets, and thus reduce the growth rate of electrode tip faces.

Acknowledgement

The authors would like to thank the support from POSCO/RIST, Korea for this study.

REFERENCES

1) M. I. Khan, M. L. Kuntz, E. Biro and Y. Zhou: Mater. Trans. **49** (2008) 1629–1637.
2) S. Fukumoto, T. Matsuo, D. Kuroda and A. Yamamoto: Mater. Trans. **49** (2008) 2844–2849.
3) GALVATECH'95. Chicago, IL: Iron and Steel Society, (1995).
4) A. Chakraborty, R. Saha and R. K. Ray: Mater. Charact. **60** (2009) 882–887.
5) A. R. Marder: Progress Mater. Sci. **45** (2000) 191–271.
6) J. M. Long, D. A. Haynes and P. D. Hodgson: Mater. Forum **27** (2004) 62–67.
7) P. Schmid, K. Uran, F. Macherey and M. Ebert: Anal. Bioanal. Chem. **393** (2009) 1863–1870.
8) C. S. Lin, M. Meshii and C. C. Cheng: ISIJ Int. **35** (1995) 503–511.
9) N. Harlin, T. B. Jones and J. D. Parker: J. Mat. Pro. Tech. **143–144** (2003) 448–453.
10) N. T. Williams, R. J. Holliday and J. D. Parker: Sci. Technol. Weld. Join. **3** (1998) 286–294.
11) F. Lu and P. Dong: Sci. Technol. Weld. Join. **4** (1999) 285–289.
12) K. L. Chatterjee and W. Waddell: Weld. Met. Fab. **64** (1996) 110–114.
13) J. E. Gould, M. Kimchi and D. H. Campbell: SAE technical paper series, 880370, (1988).
14) S. Fukumoto, I. Lum, E. Biro, D. R. Boomer and Y. Zhou: Weld. J. **82** (2003) 307s–312s.
15) T. Saito, T. Nishi and Y. Takahashi: Nippon Steel Tech. Report, **37**, Apr. (1988).
16) R. Holliday, J. D. Parker and N. T. Williams: Weld. World **37** (1996) 186–193.
17) S. J. Dong and Y. Zhou: Metall. Mater. Trans. A **34A** (2003) 1501–1511.
18) S. J. Dong, G. P. Kelkar and Y. Zhou: IEEE Trans. Electron. Pack. Manufac. **25** (2002) 355–361.
19) K. M. Pickett, J. J. Mishowski and J. E. Gould: Proc. Sheet Metal Weld. Conf. 5; AWS-Detroil Section, Detroit, MI, USA, Oct. (1992) Paper A2.
20) AWS/ANSI/SAE D8.9-97, Apr. (1997).
21) I. Lum, S. Fukumoto, E. Biro, D. R. Boomer and Y. Zhou: Metall. Mater. Trans. A **35A** (2004) 217–226.
22) L. M. Friedman and R. B. Mccauley: Weld. Res. Suppl. **48** (1969) 454s–462s.
23) P. S. James, H. W. Chandler, J. T. Evans, J. Wen, D. J. Browne and C. J. Newton: Mater. Sci. Eng. A **230** (1997) 194–201.
24) Z. Chen and Y. Zhou: Surf. Coat. Technol. **201** (2006) 2419–2430.
25) W. Tan, Y. Zhou, H. W. Kerr and S. Lawson: J. Phys. D: Appl. Phys. **37** (2004) 1998–2008.
26) U. Dilthey and S. Hicken: Weld. Cut. (1998) No. 1, 34–40.